Cooperative System with UAV and UGV for Disaster Area Exploration

Takaya Hakukawa, Kenji Uchiyama, and Kai Masuda

Abstract— **Unmanned Aerial Vehicle (UAV) and Unmanned Ground Vehicle (UGV) are expected to be widely active in exploring disaster area. However, each unmanned vehicle has problems such as short flight time or poor efficiency of the exploration. As a solution of these problems, a cooperative system between these vehicles is useful by compensating disadvantages each other. In this paper, we propose the cooperation system using quadrotor UAVs and a UGV. In the system, the potential function method that can flexibly cope with a change of environment without computational complexity is used to avoid obstacles and reach the desired position. UAVs transmit data of obstacles to a UGV so as to explore a disaster area efficiently. Super-twisting sliding mode observer (STSMO) is treated for estimating velocities of the vehicles to avoid deterioration of control performance. The validity of the proposed control system is verified through numerical simulations.**

I. Introduction

UAV and UGV have been increasingly used as a means of gathering information in disaster areas. Exploration using only a UAV is practical in that it can search efficiently in a wide range without an influence of obstacles, but it is difficult to explore for a long time because the payload is limited. Meanwhile, since a UGV is capable of lots of types of equipment such as communication device, various sensors, large battery, it can perform highly precise and long-term exploration [1]. In the case of exploration using only a UGV, the potential function method, which can flexibly respond to avoidance of obstacles without a predesigned trajectory, is useful because of light calculation load. However, depending on the parameter setting, exploration by a UGV is sometimes interrupted at a position that is a local minimum when using this method [2]. The cooperative system with a fixed-wing UAV and a UGV was proposed to overcome the problem [3]. However, this proposed method cannot fully exploit the advantages of a UAV, and UGV's obstacle avoidance depends on the parameter initial setting, therefore if obstacles have different sizes, efficient exploration cannot be done.

In this paper, we propose the cooperative system using a UGV and quadrotor UAVs. A quadrotor UAV is superior in terms of versatility and maneuverability from the viewpoint that payload restriction and low-speed flight are possible compared to a fixed-wing UAV. A UGV can supply enough power for the UAVs during a mission [4]. The advantage of the cooperative system is also to get the information such as the position and size of the obstacles from the camera mounted on the UAV and runs a better route by designing the potential function from the data. It is, however, difficult to control the system precisely and stably whenever disturbances such as wind gust and the change of running resistance. Thus, super twisting sliding mode observer (STSMO) is applied to the vehicles to estimate those velocities with robustness against disturbances acting on the vehicles. In the numerical simulation, three UAVs send data of obstacles position and size to a UGV to avoid obstacles without the interruption and perform an exploration efficiently.

The authors are with the Department of Aerospace Engineering, Nihon University, Chiba 274-8501, Japan (e-mail: csta18017@g.nihon-u.ac.jp, uchiyama@aero.cst.nihon-u.ac.jp, masuda@aero.cst.nihon-u.ac.jp).

II. Nonlinear Motion Equation And Control System

A. Control System of UAV

Nonlinear equations of motion of a UAV as shown in Fig.1 can be divided into translational motion and rotational motion. The thrust of the four propellers controls its motion. The body coordinate and the inertial coordinate systems of UAV is defined as shown in Fig. 1.

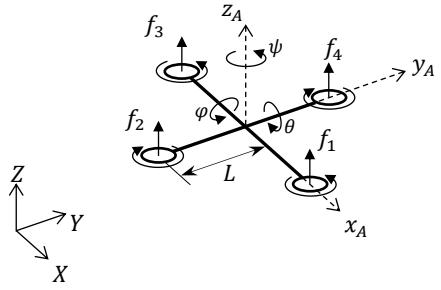

Fig. 1. Coordinate system of UAV

The UAV nonlinear dynamics [5] is linearized by using dynamic inversion (DI) method [6] to design a control system readily. The following equations express the motion of the UAV.

$$\dot{\mathbf{V}} = \frac{1}{m_A}\mathbf{F}_g - \frac{1}{m_A}k_d\mathbf{V} + \frac{1}{m_A}\mathbf{R}_{I/B}\mathbf{T} \tag{1}$$

$$\dot{\boldsymbol{\omega}} = -\mathbf{I}^{-1}\tilde{\boldsymbol{\omega}}\mathbf{I}\boldsymbol{\omega} + \mathbf{I}^{-1}\mathbf{M} \tag{2}$$

Equation (1) expresses the translational motion of the UAV in the inertial coordinate system. $\mathbf{V}$ is velocity vector, $\mathbf{R}_{I/B}$ the coordinate transformation matrix from the body-fixed coordinate system to the inertial coordinate system, $\mathbf{F}_g$ the gravitational acceleration vector in the inertial coordinate system, m_A the mass of the UAV, k_d the coefficient of air drag. $\mathbf{T}$ denotes the thrust vector generated by the four propellers of the UAV in the body coordinate system.

Equation (2) is the rotational motion of the UAV in the body-fixed coordinate system. $\boldsymbol{\omega}$ is the angular velocity vector, $\mathbf{I}$ the moments of inertia of the UAV, $\tilde{\boldsymbol{\omega}}$ a skew-

978-1-5386-8537-2/18/$31.00 ©2018 IEEE

symmetric matrix of the angular velocity vector, $\mathbf{M}$ the input vector of external torques in the body coordinate system.

Let $\mathbf{X}_A$ be the current position of the UAV and $\mathbf{X}_{Ac}$ the target position of the UAV. The position error $\boldsymbol{\varepsilon}_A$ in the inertial coordinate system is expressed as follows:

$$\boldsymbol{\varepsilon}_A = \mathbf{X}_A - \mathbf{X}_{Ac} = [X_A - X_{Ac} \quad Y_A - Y_{Ac} \quad Z_A - Z_{Ac}]^T \quad (3)$$

The second order derivative of the position error $\boldsymbol{\varepsilon}_A$ in (3) can be written as the following equation.

$$\ddot{\boldsymbol{\varepsilon}}_A = \ddot{\mathbf{X}}_A - \ddot{\mathbf{X}}_{Ac} = \dot{\mathbf{V}} \quad (4)$$

It is noted that the vector $\ddot{\mathbf{X}}_{Ac}$ is zero because the vector $\mathbf{X}_{Ac}$ is assumed to be constant. Substituting (1) into (4), then (4) can be rewritten as the equation in terms of the second order derivative of position error $\ddot{\boldsymbol{\varepsilon}}_A$ in the following equation.

$$\ddot{\boldsymbol{\varepsilon}}_A = \frac{1}{m_A}\mathbf{F}_g - \frac{1}{m_A}k_d\mathbf{V} + \frac{1}{m_A}\mathbf{T}_{I/B} \quad (5)$$

Here, the thrust $\mathbf{T}$ is transformed from the body-fixed coordinate system of the UAV to the inertial coordinate system to obtain the thrust vector $\mathbf{T}_{I/B}$ in the inertial coordinate system. The thrust vector $\mathbf{T}_{I/B}$ for linearizing the error equation by applying the DI method is expressed by the equation including nonlinear terms as follows:

$$\mathbf{T}_{I/B} = -\mathbf{F}_g + k_d\mathbf{V} + m_A\boldsymbol{\nu}_t = [T_x \quad T_y \quad T_z]^T \quad (6)$$

where $\boldsymbol{\nu}_t$ can be considered as a new control input of the linearized system. From (5) and (6), the following equation is obtained.

$$\frac{d}{dt}\begin{bmatrix}\boldsymbol{\varepsilon}_A \\ \dot{\boldsymbol{\varepsilon}}_A\end{bmatrix} = \begin{bmatrix}\mathbf{0}_{3\times3} & \mathbf{I}_{3\times3} \\ \mathbf{0}_{3\times3} & \mathbf{0}_{3\times3}\end{bmatrix}\begin{bmatrix}\boldsymbol{\varepsilon}_A \\ \dot{\boldsymbol{\varepsilon}}_A\end{bmatrix} + \begin{bmatrix}\mathbf{0}_{3\times3} \\ \mathbf{I}_{3\times3}\end{bmatrix}\boldsymbol{\nu}_t \quad (7)$$

Linear-Quadratic Regulator (LQR) is applied to the linearized motion equation. Specifically, the state feedback gain is obtained by using (7).

The Euler angle commands, φ_c and θ_c of the UAV are generated by using the components in the respective axial directions of the thrust vector $\mathbf{T}_{I/B}$ indicated by (6). Each command is expressed as follows:

$$\varphi_c = -\tan^{-1}\left(\frac{T_y}{T_z}\right), \quad \theta_c = \tan^{-1}\left(\frac{T_x}{T_z}\right), \quad \psi_c = 0 \quad (8)$$

In order to make the attitude follow its command, Euler angle error $\boldsymbol{\varepsilon}_\Phi$ is obtained from the error of a current Euler angle $\boldsymbol{\Phi}$ and desired angle $\boldsymbol{\Phi}_c$.

$$\boldsymbol{\varepsilon}_\Phi = \boldsymbol{\Phi} - \boldsymbol{\Phi}_c = [\varphi - \varphi_c \quad \theta - \theta_c \quad \psi - \psi_c]^T \quad (9)$$

The second order derivative of (9) is expressed by a rotation matrix $\mathbf{C} = \mathbf{C}(\boldsymbol{\Phi})$ and the angular velocity vector $\boldsymbol{\omega}$.

$$\ddot{\boldsymbol{\varepsilon}}_\Phi = \dot{\mathbf{C}}\boldsymbol{\omega} + \mathbf{C}\dot{\boldsymbol{\omega}} \quad (10)$$

Substituting (2) into (10), then the following equation is obtained.

$$\ddot{\boldsymbol{\varepsilon}}_\Phi = \dot{\mathbf{C}}\boldsymbol{\omega} - \mathbf{C}\mathbf{I}^{-1}\tilde{\boldsymbol{\omega}}\mathbf{I}\boldsymbol{\omega} + \mathbf{C}\mathbf{I}^{-1}\mathbf{M} \quad (11)$$

Moment vector $\mathbf{M}$ for linearizing the error equation by applying the DI method, expressed by equations including nonlinear terms as follows:

$$\mathbf{M} = -\mathbf{I}\mathbf{C}^{-1}\dot{\mathbf{C}}\boldsymbol{\omega} + \tilde{\boldsymbol{\omega}}\mathbf{I}\boldsymbol{\omega} + \mathbf{I}\mathbf{C}^{-1}\boldsymbol{\nu}_r \quad (12)$$

where $\boldsymbol{\nu}_r$ can be considered as a new control input of the linearized system. LQR is applied to the following equation obtained from (11) and (12).

$$\frac{d}{dt}\begin{bmatrix}\boldsymbol{\varepsilon}_\Phi \\ \dot{\boldsymbol{\varepsilon}}_\Phi\end{bmatrix} = \begin{bmatrix}\mathbf{0}_{3\times3} & \mathbf{I}_{3\times3} \\ \mathbf{0}_{3\times3} & \mathbf{0}_{3\times3}\end{bmatrix}\begin{bmatrix}\boldsymbol{\varepsilon}_\Phi \\ \dot{\boldsymbol{\varepsilon}}_\Phi\end{bmatrix} + \begin{bmatrix}\mathbf{0}_{3\times3} \\ \mathbf{I}_{3\times3}\end{bmatrix}\boldsymbol{\nu}_r \quad (13)$$

B. Control System of UGV

Fig.2 shows the definition of coordinate systems of a UGV. The following equations express the translational motion and rotational motions of the UGV in the body-fixed coordinate system.

$$\ddot{x} = \frac{1}{m}[-\mathrm{sgn}(\dot{x})R_x - (a_1F_1 + a_2F_2) + (F_1 + F_2)] \quad (14)$$

$$\ddot{\psi}_G = \frac{b}{J}[(a_1F_1 - a_2F_2) - (F_1 - F_2)] \quad (15)$$

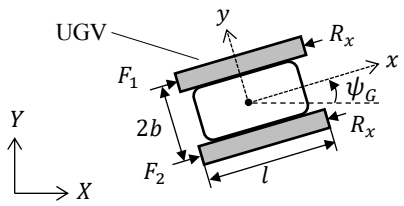

Fig. 2. Coordinate systems of UGV(top view)

In these equations, m is mass of rover, F_1 and F_2 denote forces of a crawler, J an inertial moment, b the width of UGV, and a_1 and a_2 slip ratio of the crawler, R_x running resistance of rover.

Let $\mathbf{X}_G$ be the current position of the UGV, $\mathbf{X}_{Gc}$the target position. The position error in the inertial coordinate system is defined as

$$\mathbf{X}_G - \mathbf{X}_{Gc} = [X_G - X_{Gc} \quad Y_G - Y_{Gc}]^T \quad (16)$$

where X_G and Y_G are current positions of the UGV in the inertial coordinate system. The following equation expresses the error acceleration in the body-fixed coordinate system $\ddot{\boldsymbol{\varepsilon}}_G$.

$$\ddot{\boldsymbol{\varepsilon}}_G = \mathbf{C}_{B/I}\left(\ddot{\mathbf{X}}_G - \ddot{\mathbf{X}}_{Gc}\right) = [\ddot{x}_e \quad \ddot{y}_e]^T \quad (17)$$

where $\mathbf{C}_{B/I}$ is the transformation matrix from the inertial coordinate system to the body-fixed coordinate system. Substituting (14) into (17), then the error equation of translation motion of the UGV is calculated as

$$\ddot{x}_e = \frac{1}{m}[-\mathrm{sgn}(\dot{x})R_x - (a_1F_1 + a_2F_2) + u] \quad (18)$$

Then, the thrust u, which is $F_1 + F_2$ in the body coordinate system, is obtained as follows:

$$u = \frac{1}{m}[\mathrm{sgn}(\dot{x})R_x + (a_1F_1 + a_2F_2)] + mv_x \quad (19)$$

where v_x can be considered as a new control input of the linearized system. From the equation (18) and (19), the following equation is obtained by applying LQR to the system.

$$\frac{d}{dt}\begin{bmatrix}x_e \\ \dot{x}_e\end{bmatrix} = \begin{bmatrix}0 & 1 \\ 0 & 0\end{bmatrix}\begin{bmatrix}x_e \\ \dot{x}_e\end{bmatrix} + \begin{bmatrix}0 \\ 1\end{bmatrix}v_x \quad (20)$$

The rotation controller can be designed independently of the translation controller. The heading angle error ε_ψ is defined by using the direction angle ψ_G and target direction angle ψ_{Gc}.

$$\varepsilon_\psi = \psi_G - \psi_{Gc} \quad (21)$$

Substituting the second order derivative of (21) into (15), then the following equation is obtained.

$$\ddot{\varepsilon}_\psi = \frac{b}{J}(a_1F_1 - a_2F_2) - \frac{1}{J}M_c \tag{22}$$

Here, M_c represents a moment vector in the body coordinate system. The moment vector M_c for linearizing the error equation by applying the DI method is expressed by the equation including nonlinear terms as

$$M_c = J[b(a_1F_1 - a_2F_2) + \nu_r] \tag{23}$$

where ν_r can be considered as a new control input of the linearized system (24).

$$\frac{d}{dt}\begin{bmatrix}\varepsilon_\psi \\ \dot{\varepsilon}_\psi\end{bmatrix} = \begin{bmatrix}0 & 1 \\ 0 & 0\end{bmatrix}\begin{bmatrix}\varepsilon_\psi \\ \dot{\varepsilon}_\psi\end{bmatrix} + \begin{bmatrix}0 \\ 1\end{bmatrix}\nu_r \tag{24}$$

C. Super Twisting Sliding Mode Observer (STSMO)

It is desirable for a design of a control system that all state variables of a UAV or a UGV are obtained from sensors mounted on the vehicles. Therefore, an observer is generally designed to estimate the states of the vehicles due to those payload capacities. However, disturbances such as wind gust acting on a UAV and sudden resistance change during a mission of a UGV might occur in a disaster area exploration. These disturbances result in an estimation error, deterioration of the control performance, or an interference of a mission in the worst case. It is necessary to estimate state variables with robustness against the disturbances. STSMO [7], [8] that has the robustness against the disturbances is treated to estimate those state variables. The theory and design principles are described briefly for a system.

The motion of a mechanical system including disturbance is expressed by the following equations:

$$\dot{x}_1 = x_2 \tag{25}$$

$$\begin{aligned}\dot{x}_2 &= f(x_1, x_2, u) + \xi(x_1, x_2, u) \\ u &= U(x_1, x_2)\end{aligned} \tag{26}$$

where x_1 and x_2 are arbitrary state variables. STSMO is defined by the following equation.

$$\dot{\hat{x}}_1 = \hat{x}_2 + c_1\sqrt{|x_1 - \hat{x}_1|}\mathrm{sgn}(x_1 - \hat{x}_1) \tag{27}$$

$$\dot{\hat{x}}_2 = f(x_1, \hat{x}_2, u) + c_2\mathrm{sgn}(x_1 - \hat{x}_1) \tag{28}$$

Here $\hat{x}_1$ and $\hat{x}_2$ are estimate quantities. Defining $\tilde{x}_1 = x_1 - \hat{x}_1$, $\tilde{x}_2 = x_2 - \hat{x}_2$, error equations are obtained as

$$\dot{\tilde{x}}_1 = \tilde{x}_2 - c_1\sqrt{|\tilde{x}_1|}\mathrm{sgn}(\tilde{x}_1) \tag{29}$$

$$\dot{\tilde{x}}_2 = F(x_1, \hat{x}_2, u) - c_2\mathrm{sgn}(\tilde{x}_1) \tag{30}$$

$$F(x_1, x_2, \hat{x}_2) = f(x_1, x_2, u) - f(x_1, \hat{x}_2, u) + \xi(x_1, x_2, y) \tag{31}$$

where ξ is a disturbance, c_1 and c_2 are design parameters of the observer [7]. Considering a constraint of state variables, the following inequality can be defined by using a function f^+.

$$|F(x_1, \hat{x}_2, u)| < f^+ \tag{32}$$

The parameters of observer c_1 and c_2 could be selected as $c_1 = \alpha_1\sqrt{f^+}$ and $c_2 = \alpha_2 f^+$ with constants α_1 and α_2.

The following equations represent STSMO of the UAV.

$$\begin{bmatrix}\dot{\hat{X}}_A \\ \dot{\hat{Y}}_A \\ \dot{\hat{Z}}_A\end{bmatrix} = \hat{\mathbf{V}} + c_1\begin{bmatrix}\sqrt{\tilde{X}_A}\mathrm{sgn}(\tilde{X}_A) \\ \sqrt{\tilde{Y}_A}\mathrm{sgn}(\tilde{Y}_A) \\ \sqrt{\tilde{Z}_A}\mathrm{sgn}(\tilde{Z}_A)\end{bmatrix} \tag{33}$$

$$\dot{\hat{\mathbf{V}}} = \frac{1}{m_A}\mathbf{F}_g - \frac{1}{m_A}k_d\hat{\mathbf{V}} + \frac{1}{m_A}\mathbf{T}_{I/B} + c_2\begin{bmatrix}\mathrm{sgn}(\tilde{X}_A) \\ \mathrm{sgn}(\tilde{Y}_A) \\ \mathrm{sgn}(\tilde{Z}_A)\end{bmatrix} \tag{34}$$

The estimated value of UAV velocity is obtained by (34).

On the other hand, STSMO for the UGV can be designed as

$$\begin{bmatrix}\dot{\hat{X}}_G \\ \dot{\hat{Y}}_G\end{bmatrix} = \hat{\mathbf{V}}_G + c_3\begin{bmatrix}\sqrt{\tilde{X}_G}\mathrm{sgn}(\tilde{X}_G) \\ \sqrt{\tilde{Y}_G}\mathrm{sgn}(\tilde{Y}_G)\end{bmatrix} \tag{35}$$

$$\dot{\hat{\mathbf{V}}}_G = \frac{1}{m}\begin{bmatrix}-\mathrm{sgn}(\dot{\hat{x}})R_x - (a_1F_1 + a_2F_2) + (F_1 + F_2) \\ 0\end{bmatrix} + c_4\begin{bmatrix}\mathrm{sgn}(\tilde{X}_G) \\ \mathrm{sgn}(\tilde{Y}_G)\end{bmatrix} \tag{36}$$

The velocity of the UGV in the body-fixed coordinate system is estimated by using (36).

III. Guidance Law

A trajectory of the vehicles cannot be predesigned in the disaster area because any vehicles should perform a mission in an unknown environment. The potential function method has been used to obtain a guidance law without a predesigned trajectory and calculation complexity. In this method, a gradient field of a potential function is treated as a velocity field to obtain commands for control of the vehicles.

A. Guidance of UAV

The artificial potential for the UAV consists of a steering potential function U_{sA} and a repulsive potential function U_{rA}. The following equation defines the function U_{sA} that steers the UAV for the desired position.

$$U_{sA}(\mathbf{X}) = C_{sA}\sqrt{(X_A - X_{Ad})^2 + (Y_A - Y_{Ad})^2 + L_{sA}} \tag{37}$$

where X_A and Y_A are current positions of the UAV in the inertial coordinate system. X_{Ad} and Y_{Ad} denote the desired values. C_{sA} and L_{sA} denote a design parameter for determining the maximum slope and the slope in the vicinity of the desired position, respectively.

The function U_{rA} is used for avoiding other UAVs. The equation of the potential function U_{rA} is defined in (38).

$$U_{rA}(\mathbf{X}) = C_{rA}\mathrm{e}^{-\frac{\sqrt{(X_A - X_{Ai})^2 + (Y_A - Y_{Ai})^2}}{L_{rA}}} \tag{38}$$

where X_{Ai} and Y_{Ai} are positions of other UAVs in the inertial coordinate system. C_{rA} is the magnitude of the repulsive potential, and L_{rA} a design parameter for determining the influence range.

The velocity field obtained by the potential function is derived as

$$v_{Ax} = -\frac{\partial U_{sA}(\mathbf{X})}{\partial X} - \frac{U_{rA}(\mathbf{X})}{\partial X} \quad (39)$$

$$v_{Ay} = -\frac{\partial U_{sA}(\mathbf{X})}{\partial Y} - \frac{U_{rA}(\mathbf{X})}{\partial Y} \quad (40)$$

The command of velocities and positions in (7) are generated by using (39) and (40). The height command of the UAV is also given as a constant.

B. Guidance of UGV

The potential field for the UGV consists of a steering potential function U_s, a repulsive potential function U_r, and circular potential function U_c. The following equation defines the function U_s for guiding the UGV to a destination.

$$U_s(\mathbf{X}) = C_s\sqrt{(X_G - X_{Gd})^2 + (Y_G - Y_{Gd})^2 + L_s} \quad (41)$$

where X_{Gd} and Y_{Gd} denote the desired position. C_s and L_s are design parameters like the UAV.

Next, the function U_r is defined to avoid obstacles. The size and position of the obstacle can be obtained from the UAVs. Therefore, U_r is determined by the following equation.

$$U_r(\mathbf{X}) = \|\nabla U_s(\mathbf{X})\| e^{R-\sqrt{(X_G-X_i)^2+(Y_G-Y_i)^2}} \quad (42)$$

Here, X_i and Y_i are positions of obstacles in the inertial coordinate system. R is the avoidance radius that should include an obstacle size.

The UGV can reach the desired point by using the potential field. However, it sometimes falls into a local minimum of the field or a command value generated by the field changes suddenly close to obstacles. In this case, there is a possibility that the velocity of the UGV may decrease or navigate towards a local minimum, i.e., exploration cannot be continued. We propose a new potential function U_c that is to rotate potential field to avoid local minima.

$$U_c(\mathbf{X}) = \frac{\lambda_\alpha}{1 + e^{\sqrt{(X_G-X_i)^2+(Y_G-Y_i)^2}-R}} \quad (43)$$

where λ_α is the magnitude of the circular potential. The velocity command of each axis can be obtained by following:

$$v_{Gx} = -\frac{\partial U_s(\mathbf{X})}{\partial X} - \lambda_r \frac{\partial U_r(\mathbf{X})}{\partial X} - \lambda_c \frac{\partial U_c(\mathbf{X})}{\partial Y} \quad (44)$$

$$v_{Gy} = -\frac{\partial U_s(\mathbf{X})}{\partial Y} - \lambda_r \frac{\partial U_r(\mathbf{X})}{\partial Y} + \lambda_c \frac{\partial U_c(\mathbf{X})}{\partial X} \quad (45)$$

$$\lambda_r = \frac{2}{1 + e^{\gamma\left(\sqrt{(X_G-X_i)^2+(Y_G-Y_i)^2}-R\right)}}$$

$$\lambda_c = \mathrm{sgn}\left[-(X_G - X_i)\sin\left(\tan^{-1}\left(\frac{Y_{Gd}-Y_i}{X_{Gd}-X_i}\right)\right) + (Y_G - Y_i)\cos\left(\tan^{-1}\left(\frac{Y_{Gd}-Y_i}{X_{Gd}-X_i}\right)\right)\right]$$

Here λ_r is the function that suppresses the influence region of the rotational function U_r, γ the function that determines the influence range of the function U_c. The function λ_c defines the rotational direction of the potential field.

From (46) and (47), the command of the heading angle of the UGV ψ_{Gc} in (21) is given by the following equation.

$$\psi_{Gc} = \tan^{-1}\left(\frac{v_{Gy}}{v_{Gx}}\right) \quad (46)$$

There is a possibility that the command ψ_{Gc} changes drastically when designing the repulsive potential based on the obstacle information from the UAV during a mission. The use of the function U_c contributes to the avoidance of the sudden change.

The velocity command V_{cG} and its maximum $|V_{cG}|_{max}$ of the UGV are obtained by using the function U_c. Fig. 3 shows images of these potential functions.

$$V_{cG} = \|\nabla U_s(\mathbf{x})\| \quad (47)$$

$$|V_{cG}|_{max} = \lim_{\mathbf{X}_G \to 0} \|\nabla U_s(\mathbf{x})\| \quad (48)$$

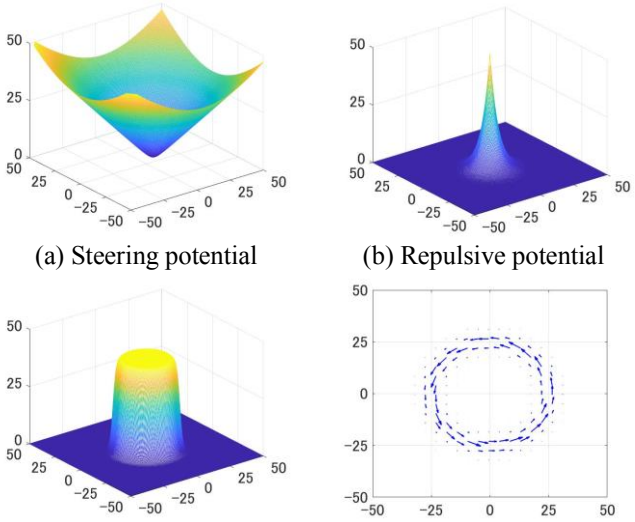

(a) Steering potential (b) Repulsive potential

(c) Circular potential and vector field

Fig. 3. Images of potential functions

IV. Cooperative Control System

If the UGV and the UAV are operated independently, there is a possibility that UGV goes away from the range of UAV's exploration. One of the solutions to the problem is to design a cooperative system using the UGV and UAVs. The UAV detects obstacles while flying ahead of the UGV and sends data of the obstacle position and size to the UGV. Fig. 4 shows the block diagram of the proposed cooperative system.

Three UAVs are used to expand the detection range of obstacles in this paper. The formation pattern of these vehicles is illustrated in Fig. 5.

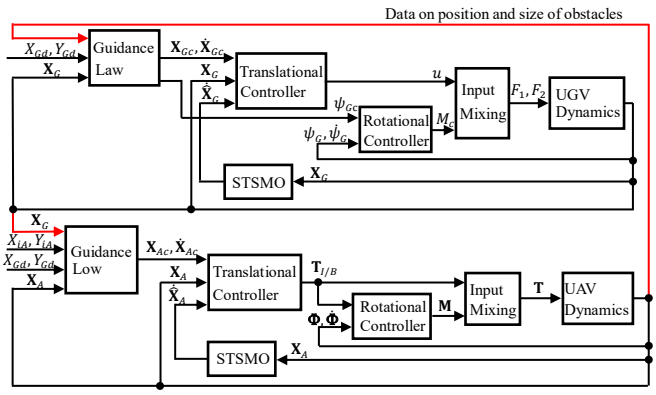

Fig. 4. Block diagram of proposed cooperative system

Desired positions of the UGV are constant. Moreover, the following equations define desired positions of the UAVs.

$$X_{Ad} = X_v + l_1 \cos\theta_1 \cos\theta_d + l_1 \cos\theta_1 \cos(\theta_d + \theta_2) \quad (49)$$

$$Y_{Ad} = Y_v + l_1 \cos\theta_1 \sin\theta_d + l_1 \cos\theta_1 \sin(\theta_d + \theta_2) \quad (50)$$

$$l_1 = 2l_r, \;\; \theta_d = \tan^{-1}\left(\frac{Y_{Gd} - Y_G}{X_{Gd} - X_G}\right)$$

where l_r is the detection range of the obstacles by on the $X-Y$ plane. θ_1 and θ_2 for UAV_1 are $\theta_1 = 0$ and $\theta_2 = 0$. For UAV_2 and UAV_3, these angles are set as $\theta_1 = \pi/4$, $\theta_2 = \pi/2$ and $\theta_1 = -\pi/4$, $\theta_2 = -\pi/2$ respectively.

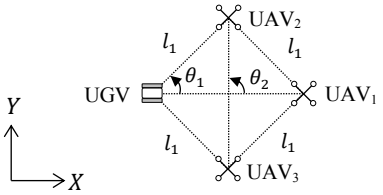

Fig. 5. Formation pattern between UAVs and UGV

V. Numerical Simulation

In the numerical simulation, the detection range l_r for three UAVs and the UGV is set to 5[m] on the $X-Y$ plane. The altitude of the UAVs is controlled at 3[m]. It is assumed that each of the UAVs and UGV can identify their position accurately. Moreover, a sensor mounted on the UAVs can detect the position and size of obstacles.

The following transfer function of dynamic characteristics of actuators is considered to simulate a more realistic environment.

$$G(s) = \frac{1}{T_a s + 1} \quad (51)$$

where T_a is a time constant of the UAVs and the UGV that is set to 0.233[s]. Furthermore, the Dryden wind turbulence model, which is a continuous gust according to stochastic processes, is used as a disturbance that acts on the UAVs. On the other hand, the resistance force acting on the UGV would vary with its position in a disaster area. The resistance force R_x is assumed to be a function of the position.

$$R_x = R_d + 0.5\sin(0.5X_G)\sin(0.5Y_G) \quad (52)$$

Here R_d, which is constant, is a running resistance obtained by adding excavation resistance and friction resistance.

Table 1 and Table 2 show the specification of the UAVs and the UGV, respectively. The design parameters of the STSMO and the potential function are shown in Table 3 and Table 4.

Fig.6(a) shows the trajectories of the UGV without obtaining the obstacle information from the UAVs. The UGV took a roundabout way to avoid the obstacle and stopped at a local minimum in the area where obstacles exist densely. It is clear from Fig.6(b) that the UGV reached the destination without any interruption by obtaining the data of obstacles from the UAVs. The UGV performed the mission efficiently by using the proposed cooperative system.

Numerical results on state variables and control inputs of these vehicles with the proposed cooperative system are shown in Fig.7. Fig.7(a) shows the time histories of the heading angle of the UGV. It took about 180 [s] to reach the desired position with avoidance of obstacles. Time responses of Euler angles of the UAV_1 are shown in Fig.7(b). The attitude of the UAV was controlled without large angle maneuver as following the UGV motion. Fig.7(c) and Fig.7(d) show result of the estimation accuracy of STSMO. The estimation error converges to zero within about 1 [s]. This result means that the STSMO is useful for estimation of velocities of the vehicles even if there exists the disturbance. Fig.7(e) and Fig.7(f) show the time histories of control inputs of the vehicles. It can be confirmed that the proposed cooperative system never requires excessive force to perform the mission.

VI. Conclusion

We designed the guidance and control system for the cooperative system using three UAVs and the UGV to explore a disaster area efficiently. The STSMO is applied to estimate velocities of the vehicles under the existence of disturbance. The potential function method is used to avoid obstacles with light calculation load. The UGV generates the potential field during a mission according to obstacles information obtained from the UAVs. Numerical results showed that the proposed cooperative system is valid for exploration.

Table 1. Specification of UAV

Mass of the UAV m_A[kg]	0.5
Radius of the UAV L[m]	0.25
Inertia about the x-axis I_{xx}[kgm^2]	5×10^{-3}
Inertia about the y-axis I_{yy}[kgm^2]	5×10^{-3}
Inertia about the z-axis I_{zz}[kgm^2]	1×10^{-2}
Air friction coefficient k_d[kg/s]	0.25

Table 2. Specification of UGV

Mass of the UGV m[kg]	0.480
Moment of inertia J[kgm^2]	5.94×10^{-3}
Length of UGV l[m]	0.150
Width of UGV L[m]	0.110
Slip ratio a_1, a_2[-]	0.1
Running resistance R_d[N]	0.19

Table 3. Parameters of the STSMO

UAV	α_1	1.5
	α_2	1.1
	f_{xA}^+, f_{yA}^+	1.1
	f_{zA}^+	1.7
UGV	α_3	1.5
	α_4	1.1
	f^+	2

Table 4. Parameters of potential function

C_{sA}	0.8	C_s	0.5
L_{sA}	10	L_s	0.3
C_{rA}	2.0	λ_α	2
L_{rA}	0.2	γ	10

REFERENCES

[1] Khaled A. Ghamry, Mohamed A. Kamel, Youmin Zhang, ''Cooperative Forest Monitoring and Fire Detection Using a Team of UAVs-UGVs'', International Conference on Unmanned Aircraft Systems, pp.1206-1211, 2016.

[2] Ryota Hatori, Kohei Shibuya, Kenji Uchiyama, ''Guidance of Exploration Rover Using Potential Function Method with Running Resistance'', Proceeding of 59th Space Science and Technology Conference, 1E03, 2015. (in Japanese)

[3] Syota Kominato, Kenji Uchiyama, ''Cooperative Control Between UAV and UGV Using Potential Field'', Proceeding of Transportation and Logistics Division Conference, 1109, 2016. (in Japanese)

[4] Davide Falanga, Alessio Zanchettin, Alessandro Simovic, Jeffrey Delmerico, Davide Scaramuzza,''Vision-based Autonomous Quadrotor Landing on a Moving Platform'', International Symposium on Safety, Security and Rescue Robotics, pp.200-207, 2017.

[5] Xin Liu, Quanmin Zhu, Pritesh Narayan, "Case Studies on U state Space Control System Design for Quadrotor Model", 8th International Conference on Modelling, Identification and Control, pp.857-862, 2016.

[6] Takahito Mikami, Kenji Uchiyama,''Design of Flight Control System for Quad Tilt-Wing UAV'', International Conference on Unmanned Aircraft Systems, pp.801-805, 2015.

[7] Junaid Anwar, Fahad Mumtaz Malik, Muhammad Abdullah, Asad Abbas, High Gain and Super-twisting Sliding Mode Observers for the Adaptive Control of Quadrotor UAV,13th International Bhurban Conference on Applied Sciences & Technology, pp.145-153, 2016.

[8] Y. Shtessel, C. Edwards, L. Fridman, and A. Levant, "Sliding Mode Control and Observation", Springer, pp.253-255, 2014.

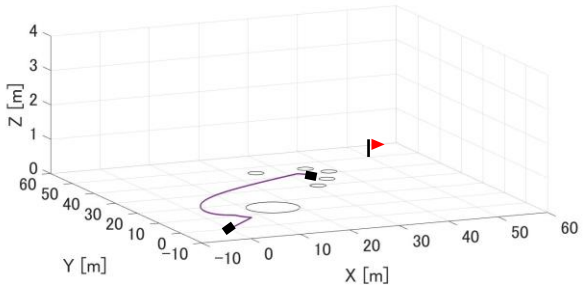

(a) Exploration using only UGV

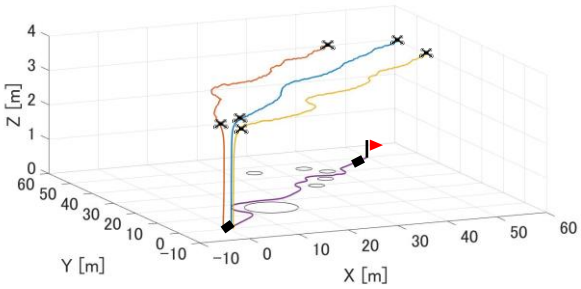

(b) Exploration using UAVs and UGV

Fig. 6. Trajectories of UAVs and UGV

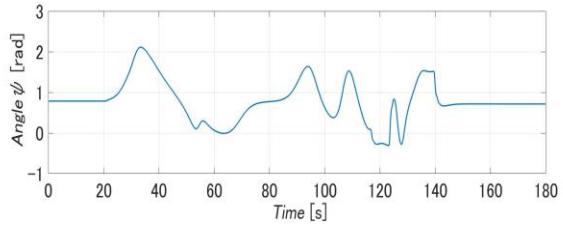

(a) Heading angle of UGV

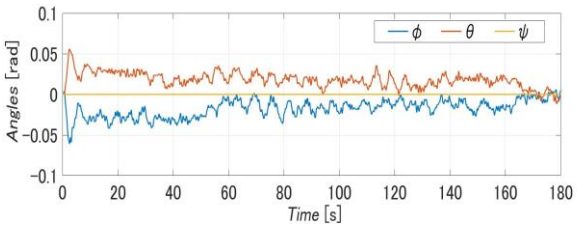

(b) Euler angle of UAV_1

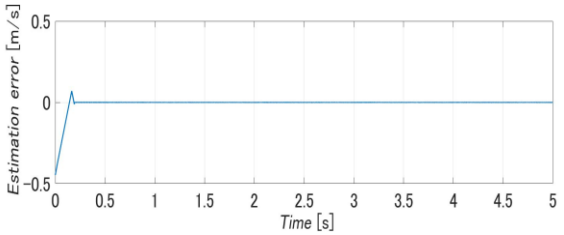

(c) Velocity estimation error of UGV

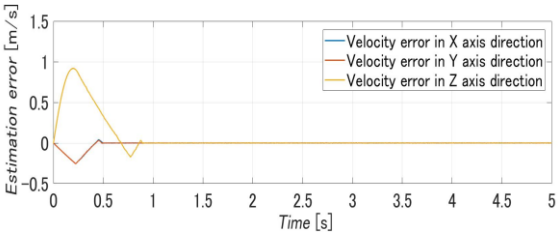

(d) Velocity estimation error of UAV_1

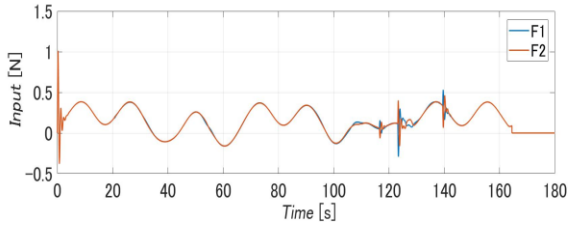

(e) Thrust of UGV at crawler

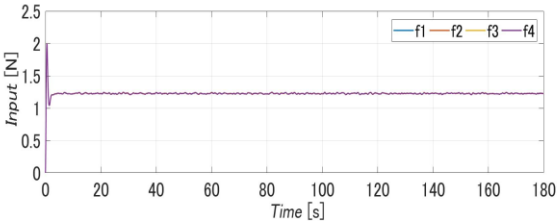

(f) Thrust of UAV_1

Fig. 7. Numerical results of UGV and UAVs with use of proposed cooperative system